PROCEEDINGS OF SCIENCE

Revisiting the chemistry of the shocked inner wind in the oxygen-rich AGB star IK Tau

David Gobrecht
Universität Basel, Switzerland
E-mail: dave.gobrecht@unibas.ch

Isabelle Cherchneff
Universität Basel, Switzerland
E-mail: isabelle.cherchneff@unibas.ch

We model shock chemistry in the inner wind of the oxygen-rich Mira star IK Tau. We describe the formation of several molecules pertaining to oxygen-rich environments using a chemical kinetic approach applied to the shocked gas layers above the stellar photosphere. The chemistry also considers the formation of metal oxides and hydrides, and dimers of SiO and AlO which are potential precursors of small silicate and alumina clusters. We perform quantum mechanic calculations to gain insight on small dust cluster structures, energetics, reaction mechanisms and finally possible formation routes. The results for the gas phase agree well with the most recent observational data for IK Tau. Major 'parent' molecules form in the shocked gas under non-equilibrium conditions and include CO, H_2O, SiO, SiS, SO, SO_2, CO_2 and HCN. In particular the model abundances of silicon- and aluminum-bearing species agree with observations, thus leaving the remaining amount of these elements available to form clusters of silicates (enstatite and forsterite) and clusters of alumina. These results indicate that 'parent' molecules and dust grains form under non-equilibrium conditions in the inner wind of IK Tau.

The Life Cycle of Dust in the Universe: Observations, Theory, and Laboratory Experiments - LCDU 2013, 18-22 November 2013
Taipei, Taiwan

PoS(LCDU 2013)093

1. Introduction

The most prolific sources of cosmic dust are Asymptotic Giant Branch (AGB) stars. In oxygen-rich AGB stars (M type, $C/O < 1$), dust grains of forsterite (Mg_2SiO_4), enstatite ($MgSiO_3$), alumina (Al_2O_3) and spinel (Mg_2AlO_4) were observed [1 – 3], but the synthesis of such dust remains poorly understood. Furthermore, large abundances of HCN and CS, which cannot be explained by thermodynamic equilibrium (TE) conditions, are found around oxygen-rich AGBs and relate to shock activity close to the photosphere [4]. In order to understand how dust grains form close to the star, we build up a non-equilibrium physico-chemical model that also reproduces the prevalent molecules in the gas-phase. In this study, we focus on the nearby galactic M-type star IK Tau which is known for its chemical diversity.

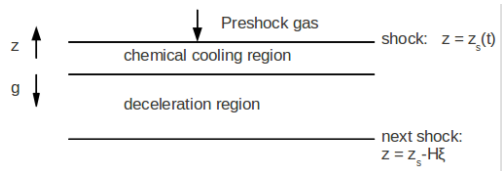

T_*	2200 K	M_*	$1M_\odot$
R_*	2.5×10^{13} cm	v_s	$20 - 32$ km/s
P	470 days	$n(1R_*)$	3.62×10^{15}cm^{-3}
r_s	$1\ R_*$	C/O	0.75

Figure 1: *Left*: Sketch of the model composed of thin chemical layer and deceleration (parcel) region. *Right:* Stellar parameters used for modeling.

2. Model

Periodic shocks induced by pulsation with velocities of 10-32 km s^{-1} enable a non-equilibrium chemistry to take place between $1R_*$ and $10R_*$ above the photosphere. The impact of shocks on the gas close to the star is modelled in two stages [5, 6]:

1. a thin 'chemical' dissociation layer corresponding to after the shock front, and
2. a hydrodynamic adiabatic cooling and deceleration region (see Figure 1).

Our best results for IK Tau are obtained for a one solar mass star of $C/O = 0.75$, shock speeds of 32 km s^{-1}, a pulsation period of $P \sim 470$ days, and the photosphere with solar abundances.
We use a chemical-kinetic approach to describe the formation of 105 molecules pertaining to oxygen-rich environments between $1R_*$ and $10R_*$. The synthesis of precursors of silicate clusters (forsterite, enstatite), metal oxides (e.g. alumina) and pure metal clusters. Density Functional Theory is a method to determine the quantum ground state of a molecule and is thus used to assess the most favourable cluster structures.

3. Results

Our modelled abundances for the prevalent species such as CO, H_2O, SiO, HCN, CS, SiS, SO, AlOH and AlO agree well with observations (see Figure 2). Our modelled abundance for SO_2 is lower by a factor 10-100. However, the observational abundance derived for SO_2 applies to the $50 - 400R_*$ region and does not trace the species in the inner wind. At these large radii, other chemical processes may be responsible for the formation of SO_2. We show that sulphur is locked

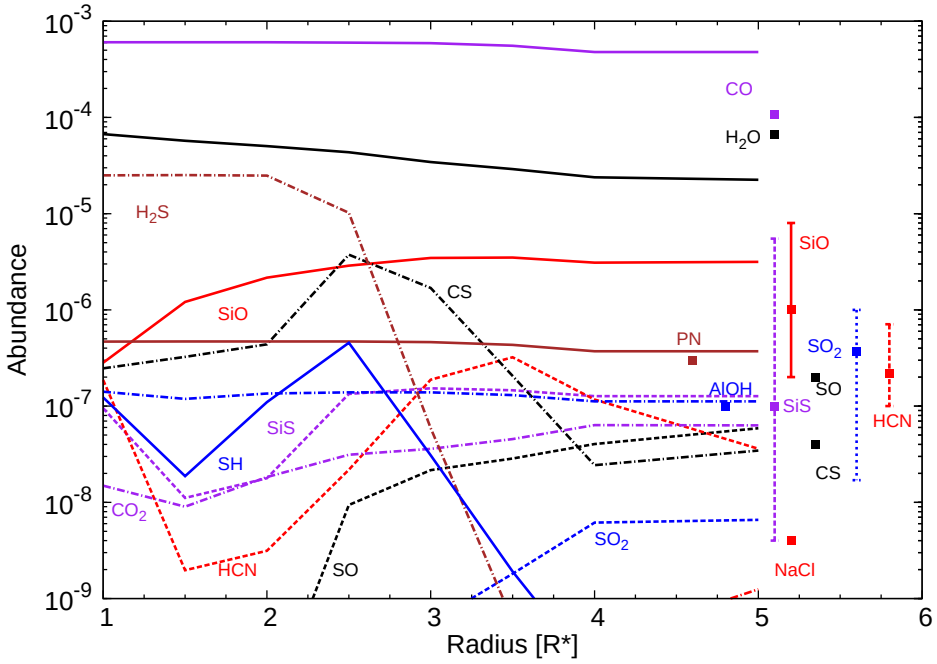

Figure 2: Gas phase molecules abundances and observational abundances (indicated by dots and error bars).

in hydrides (H_2S and SH) within $2.5R_*$, then transforms to SiS and CS and finally is found in the form of oxides (SO, SO_2) at larger radii (see Figure 2).

Our results indicate that 'parent' molecules and dust grains form in IK Tau under the non-equilibrium conditions that characterise the shocked inner region above the photosphere.

4. Conclusion and Outlook

Our findings reflect the importance of the shock-induced chemistry in the inner envelope. In future investigations we will identify pathways to enstatite ($MgSiO_3$) and forsterite (Mg_2SiO_4) as well as alumina (Al_2O_3) dimers and couple the condensation phase to the chemical kinetic nucleation phase, consider various cluster types, including spinel, and model oxygen-rich Mira stars along the AGB considering different metallicity.

References

[1] Hackwell, J. A., Gerhz, R. D., Woolf, N. J. 1970, *Nature*, 227:822-823

[2] Onaka, T., de Jong, T., Willems, F. J. 1989, *A&AS*, 81:261-284

[3] Posch, T., Kerschbaum, F., Mutschke, H., et al. 1999, *A&A*, 352:609-618.

[4] Duari, D., Cherchneff, I., Willacy, K. 1999, *A&A*, 341:L47–L50.

Table 1: Predicted abundances (with respect to H_2) of selected species: Given TE (Thermodynamic Equilibrium) abundances at $1R_*$, modelled abundances at $5R_*$ and observed abundances.

Species	TE($1R_*$)	Modelled ($5R_*$)	Observed	Reference
CO	8.06×10^{-4}	1.07×10^{-3}	1.0×10^{-4}	[7] + ref. therein
H_2O	1.87×10^{-4}	6.17×10^{-5}	6.6×10^{-5}	[8]
SiO	7.48×10^{-5}	2.00×10^{-5}	$8.0 \times 10^{-6} - 2.0 \times 10^{-7}$	[7] + ref. therein
HCN	7.20×10^{-11}	1.33×10^{-7}	$(1.5 - 7.1) \times 10^{-7}$	[9], [7] + ref. therein
CO_2	2.91×10^{-8}	1.63×10^{-7}	5.9×10^{-8}	[10]
CS	1.61×10^{-10}	3.07×10^{-8}	4.0×10^{-8}	[7] + ref. therein
SiS	3.27×10^{-7}	1.90×10^{-7}	$5.5 \times 10^{-6} - 4.0 \times 10^{-9}$	[7] + ref. therein
SO	2.54×10^{-8}	1.60×10^{-7}	2.0×10^{-7}	[7] + ref. therein
SO_2	6.69×10^{-12}	2.02×10^{-8}	1.0×10^{-6}	[7] + ref. therein
H_2S	7.62×10^{-7}	3.79×10^{-12}	1.0×10^{-5}	[11]
SH	6.94×10^{-6}	6.84×10^{-12}	1.0×10^{-7}	[12]
NaCl	1.21×10^{-11}	2.80×10^{-9}	4.0×10^{-9}	[13]
HCl	3.77×10^{-7}	2.22×10^{-7}	1.0×10^{-8}	[12]
AlO	5.68×10^{-9}	4.62×10^{-10}	6.0×10^{-9}	[14], [15]
AlOH	1.23×10^{-8}	2.53×10^{-7}	1.0×10^{-7}	[16]
PN	1.08×10^{-9}	5.67×10^{-7}	3.0×10^{-7}	[17]
PO	7.32×10^{-8}	1.13×10^{-7}	$(0.5 - 3.0) \times 10^{-7}$	[17]
TiO	1.91×10^{-7}	2.20×10^{-7}	2.51×10^{-9}	[18]
TiO_2	9.07×10^{-13}	4.19×10^{-8}	3.16×10^{-10}	[18]

[5] Cherchneff, I., 2006, *A&A*, 456:1001–1012.

[6] Cherchneff, I., 2012, *A&A*, 545:A12

[7] Decin, L., De Beck, E., Brünken, et al. 2010, *A&A*, 516:A69.

[8] Decin, L., Justtanont, K., De Beck, E., et al. 2010, *A&A*, 521:L4.

[9] Schöier, F. L., Ramstedt, S., Olofsson, H., et al. 2013, *A&A*, 550:A78

[10] Markwick, A. J., Millar, T. J. 2000, *A&A*, 359:1162-1168

[11] Omont, A., Lucas, R., Morris, M., Guilloteau, S. 1993, *A&A*, 267:490–514.

[12] Yamamura, I., Kawaguchi, K., Ridgway, S. T. 2000, *APJL*, 528:L33–L36.

[13] Milam, S. N., Apponi, A. J., Woolf, N. J., et al. 2007, *APJL*, 668:L131–L134.

[14] Tenenbaum, E. D., Ziurys, L. M. 2009, *APJL*, 694:L59–L63.

[15] Kamiński, T., Schmidt, M. R., Menten, K. M. 2013, *A&A*, 549:A6.

[16] Tenenbaum, E. D., Ziurys, L. M. 2010, *APJL*, 712:L93–L97.

[17] De Beck, E., Kamiński, T., Patel, et al. 2013, *ArXiv e-prints*, in:prep.

[18] Kamiński, T., Gottlieb, C. A., Menten, K. M., et al. 2013, *A&A*, 551:A113.

[19] Kim, H., Wyrowski, F., Menten, K. M., Decin, L. 2010, *A&A*, 516:A68.